Lumped element model of THORNT and PMHS abdomen under seatbelt and impactor loading

Romain Desbats, François Bermond, Sabine Compigne, Stéphane Nicolle, Philippe Vezin

Lumped element model of THOR-NT and PMHS abdomen under seatbelt and impactor loading

Romain Desbats, François Bermond, Sabine Compigne, Stéphane Nicolle, Philippe Vezin

Abstract Abdominal injuries represent a small proportion of crash injuries but it increases considerably with regard to serious to severe injuries. It is important to assess abdomen injury risk using a biofidelic crash test dummy, especially under seatbelt loading. A lumped element model has been used to simulate seatbelt and impactor loading cases on Post Mortem Human Subjects (PMHS) subject and on the THOR dummy. The model consists of two blocks of one spring and one damper with a mass between the blocks and a mass at the front of the model. The front block has the spring and damper in series, whereas they are in parallel for the rear block, to reproduce the abdomen and back force respectively. The mechanical parameters of the model have been optimised to fit the force-penetration response of PMHS and of the dummy. The results show that the PMHS response is more damper-dependent, whereas the dummy response is more spring-dependent. Moreover, unlike the PMHS, the THOR dummy model needs a non-linear spring in order to fit the impactor test data. The conclusions are that the dummy abdomen should be modified to make it more viscously deformable and to include pelvis design modifications in order to prevent a too stiff response.

Keywords abdomen response, biofidelity, lumped element model, THOR dummy

I. INTRODUCTION

Abdominal injuries represent only a small proportion of all injuries caused by car crashes compared to those of the head, chest or limbs, but their proportion increases considerably with regard to serious to severe injuries (AIS 3 or more): 8% of AIS3+ injuries, 16.5% of AIS4+ injuries and 20.5% of AIS5+ injuries [1]. Besides, it is also shown that rear occupants have a 1.7 times higher risk of suffering an injury to the abdomen than front occupants [2]. Therefore, to provide the best protection to all car occupants, assessing the risk of abdominal injury using a biofidelic crash test dummy is important, especially under seatbelt loading known to be the most common source of AIS3+ injuries to the digestive system [1]-[3].

Abdomen biofidelity of crash test dummies under seatbelt loading is not included in biofidelity targets. The biofidelity of the THOR dummy proved to be limited under seatbelt and impactor loadings, as shown in [4] and [5] where force-penetration responses of the THOR-NT (reprocessed data from [6]) were compared to PMHS corridors. Two impactor conditions and two seatbelt conditions were considered in [5]. For the impactor cases, the dummy response is above the PMHS corridors after 80 mm whereas for the seatbelt cases, the dummy response is below the PMHS corridors. Finite element models, as well as lumped element models, are tools to help the analysis of human surrogates abdomen response such as PMHS and dummy. The first lumped element model developed to simulate human behaviour under impact is the thorax model from [7]. Reference [8] used this model to simulate an impactor loading case, as well as a seatbelt loading case to the thorax. A simplified version of the same model was used in [9], where the mechanical parameters were optimised to match a given thoracic response. A lumped element model was used to describe the abdomen response under seatbelt tests in [4]. The model consisted of a spring in parallel with a damper and a mass at the front for the dummy case only. The mass value was tuned to fit THOR dummy abdomen behaviour. The PMHS version of this model was enhanced in [10]: a second stage was added to the model, linked with a mass to the first one. This allowed modelling the force between the subject and the back support of the test bench during a seatbelt test.

R. Desbats is Ph.D. student in Biomechanics, F. Bermond (email: francois.bermond@ifsttar.fr, Tel. +33 4 72 14 23 78) is researcher, S. Nicolle is Associate Professor and P. Vezin is senior researcher at Université de Lyon - IFSTTAR. S. Compigne is technical manager at Toyota Motor Europe NV/SA.

The objective of this study is to continue the study from [4] with more loading conditions and to quantify the biofidelity of the THOR dummy through a comparative analysis of the responses to seatbelt and impactor loadings of the PMHS and the THOR dummy. A common lumped element model will be used to reproduce the PMHS and THOR responses by optimising the model's mechanical parameters. The use of a lumped element model allows to identify mechanical properties more quickly than a FE model, due to a shorter computation time and the reduced number of parameters. The differences between the PMHS and the THOR responses could be explained and quantified by the variations between parameters values.

II. METHODS

Test data

Seatbelt

The seatbelt tests selected from the literature and applied to the lumped element model are taken from [8-10] for the PMHS tests and from [5] (replication of tests from [11]) and [4] for the THOR dummy. These are fixed-back tests where the belt is placed on the abdomen at the umbilicus level and retracted toward the back of the subject thanks to pretensioners (or by a piston for one of two condition in [10]). Three conditions from the literature are common to PMHS subjects and the dummy: B and C conditions from [11] (different pretensioners) and condition 2 from [4].

For the PMHS tests, the average penetration across all the subjects for a given condition was applied to the model. The average force was compared to the model response. Two tests were performed for each condition in [5]. The average penetration of those two tests was computed, differentiated to obtain velocity and then differentiated a second time to determine acceleration. The three signals were filtered in order to avoid noise that would distort the model computations. Average penetration, velocity and acceleration were applied to the model and the average force was compared to the model response. One test per condition was performed in [4]. Fig. 1 shows those input conditions applied to the lumped element model overlaid together. It can be seen that all the input conditions do not have the same time duration and for some of them the data is not available over the full time range of the test.

Impactor

Six impactor conditions were applied to the model. For the PMHS subjects, two conditions were taken from [12] and [13]. The tests with a 64 kg mass from [12] have been excluded. For the THOR dummy two conditions were taken from [5]. There is only one common configuration for the PMHS and the dummy, the 6 m/s (nominal velocity) 32 kg test condition. For each configuration, the penetration data from the different tests were averaged and the corresponding initial velocity was taken as input condition v_0. Table I shows the considered input velocities.

TABLE I

INITIAL IMPACT VELOCITY VALUES

	condition	v_0 (m/s)	m_i (kg)	kinetic energy (J)
PMHS	Cavanaugh et al. 1986 6.1 m/s	6.1	32	595
	Cavanaugh et al. 1986 10 m/s	10	32	1600
	Hardy et al. 2001 6 m/s	6.5	48	1028
	Hardy et al. 2001 9 m/s	8.5	48	1745
THOR	Compigne et al. 2015 3 m/s	3.0	32	141
	Compigne et al. 2015 6.1 m/s	6.3	32	628

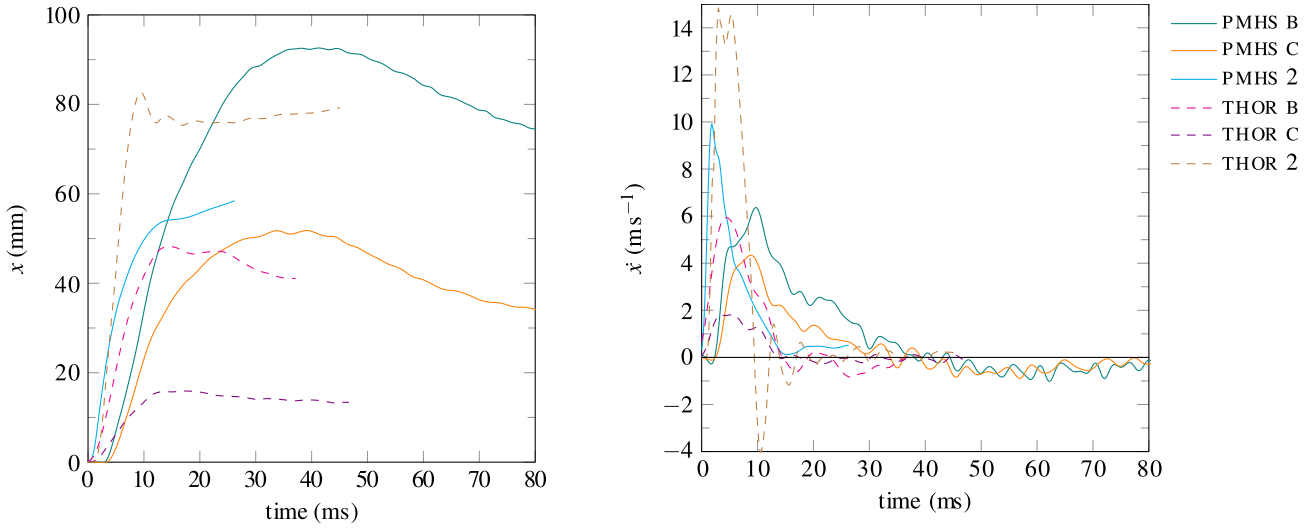

(a) Abdomen penetration. (b) Abdomen penetration velocity.

Fig. 1. Input conditions for seatbelt loading conditions common to the PMHS and the THOR dummy.
B: B condition from Foster et al. 2006
C: C condition from Foster et al. 2006
2: configuration 2 from Trosseille et al. 2002

Lumped element model

A lumped element model was used to reproduce PMHS and THOR-NT force-penetration responses, in order to compare the mechanical parameters creating this response. The two stages of the model are meant to represent the behaviour of the organs, on one hand, and of the flesh and skin, on the other hand. Each stage of this model consists of a spring associated with a damper in order to represent a visco-elastic behaviour. This model is based on the work of [10], with some modifications. Linear elements were used instead of components with a cubic relationship, and a mass has been added at the front of the model to represent the flesh and skin mass. A mass has also been added at the back of the model to represent the global subject mass. This mass is fixed to model a seatbelt loading and let free to model an impactor test. An important modification of the structure of the model was carried out in order to represent both seatbelt and impactor loading cases. Indeed, the original model from [10] had the springs and dampers in parallel (Kelvin-Voigt model) and therefore could model a seatbelt test but not an impactor test. Since the extremity of the model has a non-zero initial velocity, the fact of having a damper in parallel created a non-zero initial reaction force. This is in contradiction with the test data. Therefore, it was chosen to transform the front stage of the model into a spring in series with a damper (Maxwell model). Fig. 2 shows the models for seatbelt and impactor loading cases.

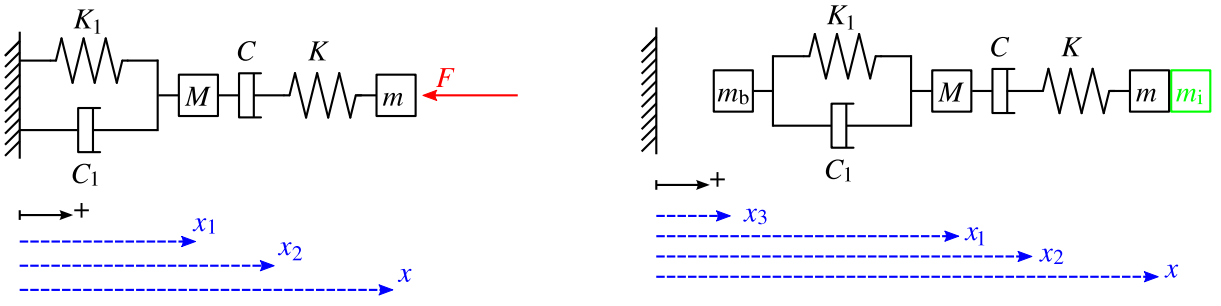

(a) Seatbelt. (b) Impactor.

Fig. 2. Simplified abdomen model for seatbelt and impactor loading cases.

Model equations and resolution

Seatbelt

The variables of the model can be seen on Fig. 2(a). It was chosen to impose the x displacement and its derivatives $\dot{x}$ and $\ddot{x}$ as input conditions. The model response was considered as the force F. They are taken from the test data and imposed on the model. Equations 1(a) and 1(b) are the equations of motion of the system, obtained by isolating the mass M and the point where x_2 is measured (massless node linking the spring and the damper in series), respectively.

$$\begin{aligned} -M\cdot\ddot{x}_1 &= K_1\cdot x_1 + C_1\cdot\dot{x}_1 - C\cdot\left(\dot{x}_2-\dot{x}_1\right) && \text{(a)} \\ 0 &= -K\cdot\left(x-x_2\right)+C\cdot\left(\dot{x}_2-\dot{x}_1\right) && \text{(b)} \end{aligned} \tag{1}$$

Equations 1(a) and 1(b) are two coupled differential equations where the unknowns are x_1 and x_2 and where x_2 is used to compute F from Equation 2 (obtained from isolating the mass m) and x_1 is used to compute the force between the back of the subject and the test bench, as shown on Equation 3.

$$F = m\cdot\ddot{x} + K\cdot\left(x-x_2\right) \tag{2}$$

$$F_{\text{back}} = K_1\cdot x_1 + C_1\cdot\dot{x}_1 \tag{3}$$

Impactor

The model for impactor case is detailed on Fig. 2(b). The initial impactor velocity, $v_0 = \dot{x}(t=0)$, is imposed to the model. Equations 4(a) to 4(d) give the equations of motion of the model. The interaction force between the impactor and the subject is computed according to Equation 5. The differential equations systems are solved with a Runge-Kutta method programmed in the Scilab software.

$$\begin{aligned} -\left(m+m_{\text{i}}\right)\cdot\ddot{x} &= K\cdot\left(x-x_2\right) && \text{(a)} \\ 0 &= -K\cdot\left(x-x_2\right)+C\cdot\left(\dot{x}_2-\dot{x}_1\right) && \text{(b)} \\ -M\cdot\ddot{x}_1 &= -C\cdot\left(\dot{x}_2-\dot{x}_1\right)+K_1\cdot\left(x_1-x_3\right)+C_1\cdot\left(\dot{x}_1-\dot{x}_3\right) && \text{(c)} \\ -m_{\text{b}}\cdot\ddot{x}_3 &= -K_1\cdot\left(x_1-x_3\right)-C_1\cdot\left(\dot{x}_1-\dot{x}_3\right) && \text{(d)} \end{aligned} \tag{4}$$

$$F = \left(m+m_{\text{i}}\right)\cdot\ddot{x} \tag{5}$$

Cubic non-linear element as used in [10] proved to be difficult to use in this study: a cubic stiffness has little effect on small compression values but great effect on higher compression values due to the nature of the cubic relation. It was therefore difficult to fit all the test data with such elements. Good non-linear components would include more than one parameter in order to amplify differently low and high compression values. It was therefore decided to use only linear components in the model, if they are sufficient to fit the test data, so as not to add parameters to the model if not necessary. However, it was not possible to fit the THOR dummy impactor test data with linear elements. It was therefore decided to replace the element K with a non-linear spring that shows a strain dependence as seen in Equation 6. The nonlinear stiffness browses successively two regimes of compression and is characterised by three parameters: a linear stiffness K_0; a compression limit d; and a power p (imposed as an integer number). For low compression values, when $\left(x-x_2\right) << d$, the term between curly brackets in Equation 6 reduces to unity and the response of the spring is linear, $F_{\text{spring}} = K_0\cdot\left(x-x_2\right)$. At moderate to high compression, a stiffening sets in and the restore force becomes higher than the K_0 linear contribution.

$$F_{\text{spring}} = K_0\cdot\left(x-x_2\right)\cdot\left\{1+\left(\frac{\left|x-x_2\right|}{d}\right)^p\right\} \tag{6}$$

Determination of model parameters

Masses determination

Due to the abdomen representation described above, the masses of the model had to be estimated for the human subjects. It was chosen to use the THUMS model described in [14] to measure those masses. The THUMS model has a representation of the abdomen internal geometry and densities for a 50th percentile male (175 cm height, 77 kg mass) which allows to estimate the masses repartition according to the lumped element model structure. The abdomen was isolated from the rest of the model by drawing a 3D box between L1 and L5 lumbar vertebrae. The abdomen was divided in three areas as shown on Fig. 3. The *abdomen content* area is meant to represent the organs that will move during the impact and will correspond to the mass M in the simplified model. The *front flesh* area represents the tissues that create the initial inertia of the abdomen when subjected to seatbelt loading and corresponds to the mass m. The *back* area represents the back of the subject (including the spine) that deforms little during the compression of the abdomen. However, the mass m_b, which is used only in an impactor test condition, would be greater than the mass of the *back* area since more than this body part moves during a free back impact. The calculated masses on the THUMS model (from the selected parts densities) are M = 5.7 kg and m = 0.92 kg.

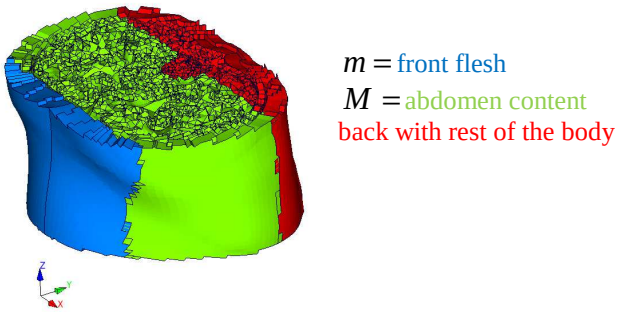

Fig. 3. Masses repartition of the THUMS model.

Therefore, M = 6 kg and m = 1 kg were used for all the PMHS subjects. An exception was made for configuration 2 from [4], where m has been set to 0.5 kg due to the low body mass of the PMHS subjects (45 kg and 50 kg). Table A.III. (see Appendix) presents the anthropometry of the considered PMHS subjects. The mass m_b was computed as $m_b = BM - M - m$, where BM is the average body mass of the PMHS subjects of the considered test condition. The masses for the THOR dummy were measured on the dummy v1.0 FE model (see [15] for v0.0). The part densities were taken from [16]. The mass of the two foam blocks of the abdomen together is approximately 0.3 kg. Therefore, M was set to 0.2 kg and m was set to 0.1 kg. The mass m should also account for a portion of the dummy jacket, but it is not possible to estimate this contribution. The mass m_b was computed as m_b = 78.3 kg $- M - m$ = 78 kg, since the total mass of the dummy is equal to 78.3 kg according to [17].

Optimisation loop

The response of the model for a specific loading condition is computed with a Scilab program. Based on manually adjusted initial values, the parameters values are optimised for each test configuration with the Scilab "optim" function until the model response (the force signal) matches the test data, minimising the criteria $f = \sum_{i=1}^{N} \left(F_{\text{model}}(i) - F_{\text{test}}(i)\right)^2$ with N the number of data points. The goodness of fit is then estimated by calculating cross-correlation coefficients and the variation range of the parameters is determined.

Goodness of fit assessment

The assessment of the goodness of fit between the model response and the reference test data is obtained by

calculating amplitude ratio, shape factor and phase shift as described in [18]. Equations 7(a) to 7(c) define the three ratios with $x(t)$ being the signal to compare to the reference $y(t)$ and $\|x\| = \int_{-\infty}^{+\infty} x^2(t) \cdot \mathrm{d}t$ the norm of x. The integrals of digital signals are computed as: $\int_{-\infty}^{+\infty} x(t) \cdot \mathrm{d}t = \sum_{i=1}^{N-1} T \cdot \frac{x_{i-1} + x_i}{2}$ with T the sampling rate (numerical integration by trapezoidal rule). A perfect fit between the two signals would lead to an amplitude ratio and a shape factor of 1 and a phase shift of 0.

$$\text{amplitude ratio} = \frac{\|x\|}{\|y\|} \qquad \text{(a)}$$

$$\text{shape factor} = \frac{\int_{-\infty}^{+\infty} x(t) \cdot y(t) \cdot \mathrm{d}t}{\sqrt{\|x\| \cdot \|y\|}} \qquad \text{(b)} \qquad (7)$$

$$\text{phase shift} = h \text{ so that } \frac{\int_{-\infty}^{+\infty} x(t) \cdot y(t+h) \cdot \mathrm{d}t}{\sqrt{\|x\| \cdot \|y\|}} \text{ is minimal} \qquad \text{(c)}$$

Sensitivity analysis

In order to compare the model parameters for different conditions, it was necessary to estimate the range in which the optimised parameters can vary without significantly changing the model response result. The optimised values of the model parameters (spring stiffnesses and damping parameters) and the masses values were subjected to variations by steps of 10% of their value, ranging from 0.1 to 2 times the initial value. For each parameter value the three correlation coefficients mentioned above between the model response and the test data were computed. The percentage of variation of the three coefficients was computed at each step. A variation of one of the coefficients exceeding 10% of the coefficient value computed with the optimised parameter was considered as the limit of the range of variation of the parameter. An exception was made for the phase shift coefficient. In order to avoid the artefacts due to small phase values, the value of phase shift used in these computations was divided by 10 ms and the coefficient $1 - \frac{\text{phase shift}}{10\ \text{ms}}$ was considered instead of the phase shift in ms, in order to have a coefficient equal to 1 in case of a perfect fit.

III. RESULTS

Model fit to test data

Figures 4 and 5 show the model response fit to the test data under seatbelt and impactor loading respectively, for the common conditions between PMHS subjects and the dummy. This model response is obtained with the optimised mechanical parameters values reported in Tables A.I. and A.II., respectively (see Appendix). Non-normalised data have been used for the PMHS penetration and force response. The standard deviation corridors are indicated for the PMHS force data. The goodness of fit coefficients are reported at the bottom of each subfigure. Force-penetration graphs of those results are presented in Fig. A.1. (see Appendix).

For the seatbelt conditions, the initial negative slope of the model force response for some tests is an artefact due to the negative slope in the $\dot{x}$ data (see Fig. 1(b)). This may be a consequence of the filtering of penetration data to compute the input velocity. The THOR dummy response shows sharp peaks and an abrupt initial slope that the model can-not fit exactly, regardless of the potential time offset in the force signal from test data. For the impactor conditions, The non-linearity of the dummy response can be seen on Fig. 5(c) and (d), where the slope of the force-time signal changes around 10 ms, and on Fig. A.1. (c) and (d). Comparing Figures A.1. (c) and (d) for the PMHS data, it appears that the model predicts a higher penetration than measured in the test data.

For both seatbelt and impactor case the model allows to fit the test data, the response being mainly in the standard deviation corridors for the PMHS, the amplitude and shape ratios stay between 0.8 and 1.1 and the phase shift between ±1.2 ms. This means that this model is suitable to analyse the human and dummy abdomen response.

Parameters values

Figure 6 shows the parameters identified for each common PMHS/dummy condition along with their range of variation for the seatbelt and impactor cases, respectively. The numerical values are reported in Table A.I. and Table A.II. (see Appendix).

For the seatbelt case, the first thing to be noticed on Fig. 6(a) is that the K values for the PMHS subjects are much higher than for the THOR dummy. The C values are higher for the dummy than for the PMHS subjects (Fig. 6(c)), except for configuration 2 from [4] where they are equal. The C_1 values (Fig. 6(g)) are higher for the dummy compared to the PMHS, except for the configuration 2 from [4], but since ranges of variation overlap for most of the test conditions, it is concluded that the C_1 values are the same for the PMHS and the dummy. Additionally, the K_1 values presented on Fig. 6(e) are similar between the PMHS and the dummy, but large ranges of variation exist for all of the conditions. This high range of variation of the parameter K_1 is due to the fact that x_1 is significantly lower than x for most of the conditions. Therefore, a given variation of K_1 would have less effect on the abdomen force than the same variation of K. Regarding the results for configuration 2 from [4], the fact that C is equal for the PMHS and the dummy and that C_1 is lower for the dummy, can be explained by the fact that the penetration velocity is the highest for this condition (Fig. 1(b)).

For the impactor case, since a non-linear spring was needed to fit the THOR test conditions, the effective stiffness of these conditions is compared to the K values of the other conditions on Fig. 6(b). The effective stiffness for the non-linear spring is computed as $K_{eff} = \frac{F_{spring}}{x - x_2}$ with F_{spring} taken from Equation 6, the force given by the spring. K_{eff} is plotted against the relevant elongation, $x - x_2$. For a linear spring (PMHS case), $K_{eff} = K$. For clarity, only optimised values are plotted, without range of variation. The K_{eff} values for the THOR dummy are lower than the K values of the PMHS subjects on most of the penetration range. The C values are higher for the THOR dummy compared to the PMHS subjects (Fig. 6(d)) except for 10 m/s condition where the PMHS have a higher C value than the other conditions. The same trend is noted for the C_1 parameter (Fig. 6(h)), although there is a large range of variation for the 10 m/s condition. The K_1 values presented on Fig. 6(f) seem higher for the dummy compared to the PMHS, but due to relatively large ranges of variation of this parameter it can take the same values for all the conditions. The same observation can be made for the high range of variation of K_1 than in the seatbelt case. The fact that the 10 m/s condition has a higher C value compared to the other PMHS condition can be due to the fact that this is the highest velocity of the test conditions.

It stands out that the second stage of the model contributes less to the global penetration response of the model since the displacement and velocity of the second stage, (x_1 and $\dot{x}_1$ for seatbelt, $x_1 - x_3$ and $\dot{x}_1 - \dot{x}_3$ for impactor), are lower than those of the front stage ($x - x_1$ and $\dot{x} - \dot{x}_1$). This leads to focussing on the K and C parameters for the analysis.

For the conditions that are not common to the PMHS and the dummy, the optimised parameters are presented in Fig. A.2. (see Appendix). The same trends and order of magnitudes as explained above can be noticed.

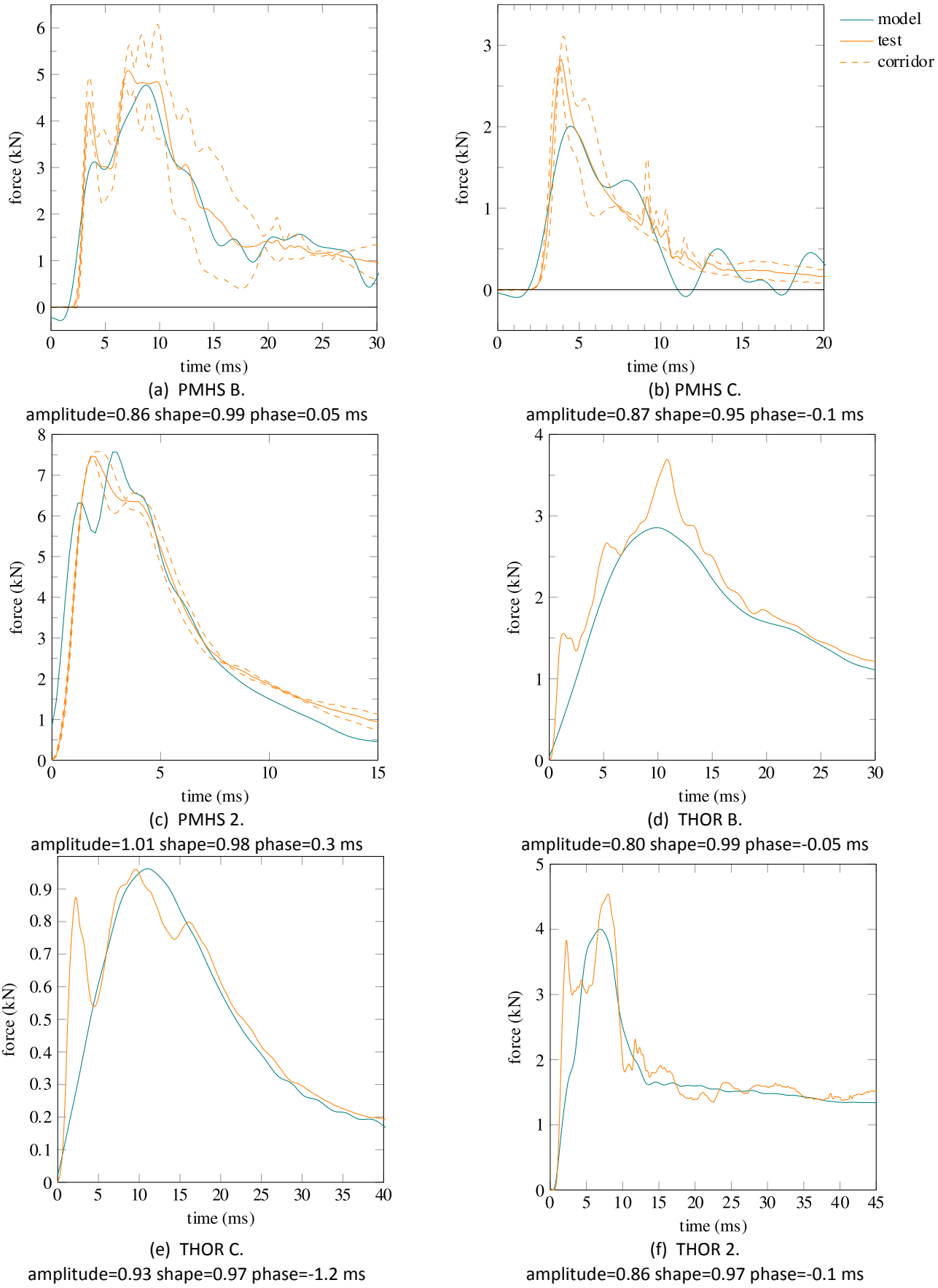

(a) PMHS B.
amplitude=0.86 shape=0.99 phase=0.05 ms

(b) PMHS C.
amplitude=0.87 shape=0.95 phase=-0.1 ms

(c) PMHS 2.
amplitude=1.01 shape=0.98 phase=0.3 ms

(d) THOR B.
amplitude=0.80 shape=0.99 phase=-0.05 ms

(e) THOR C.
amplitude=0.93 shape=0.97 phase=-1.2 ms

(f) THOR 2.
amplitude=0.86 shape=0.97 phase=-0.1 ms

Fig. 4. Fit of the model response to test data for seatbelt case.
B: B condition from Foster et al. 2006
C: C condition from Foster et al. 2006
2: configuration 2 from Trosseille et al. 2002

265

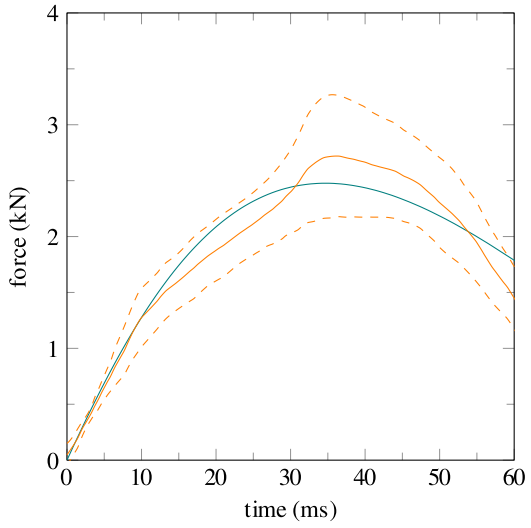

(a) PMHS 6.1 m/s.
amplitude=0.95 shape=1.00 phase=0 ms

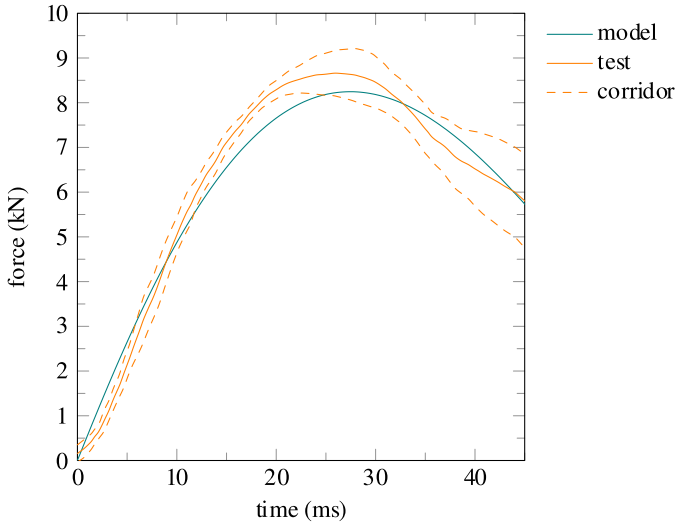

(b) PMHS 10 m/s.
amplitude=1.00 shape=1.00 phase=0 ms

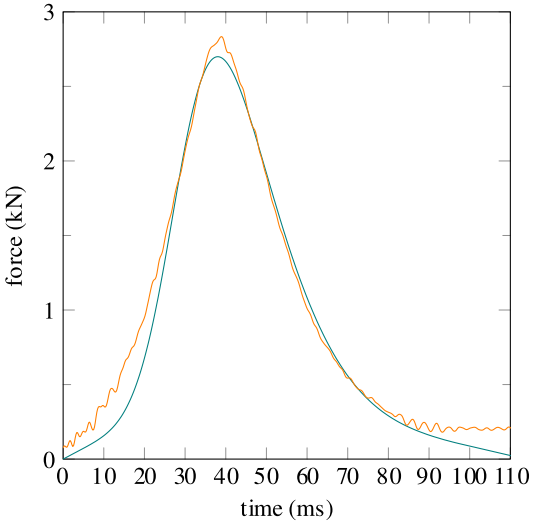

(c) THOR 3 m/s.
amplitude=0.94 shape=0.99 phase=-1 ms

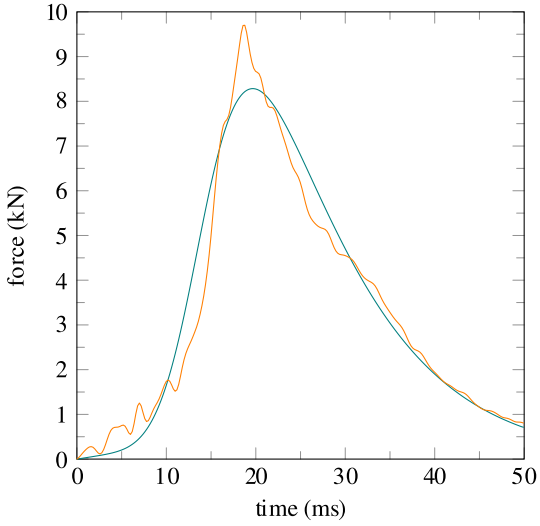

(d) THOR 6.1 m/s.
amplitude=1.04 shape=0.99 phase=0.4 ms

Fig. 5. Fit of the model response to test data for impactor case.
PMHS 6.1 m/s: 32 kg 6.1 m/s condition from Cavanaugh et al. 1986
PMHS 10 m/s: 32 kg 10 m/s condition from Cavanaugh et al. 1986
THOR 3 m/s: 32 kg 3 m/s condition from Compigne et al. 2015
THOR 6.1 m/s: 32 kg 6.1 m/s condition from Compigne et al. 2015

266

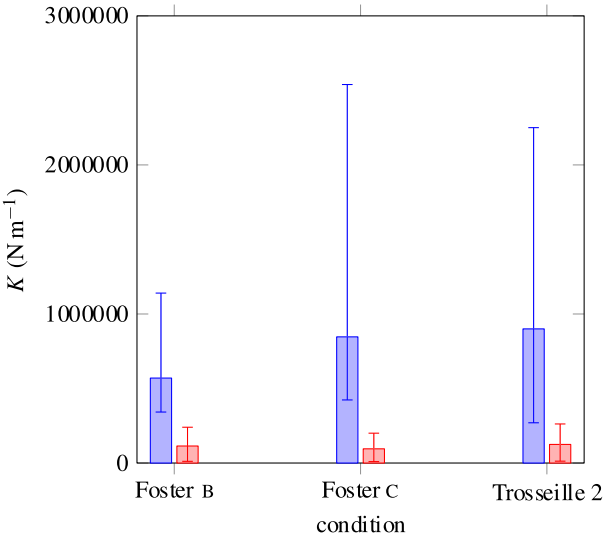

(a) K for seatbelt.

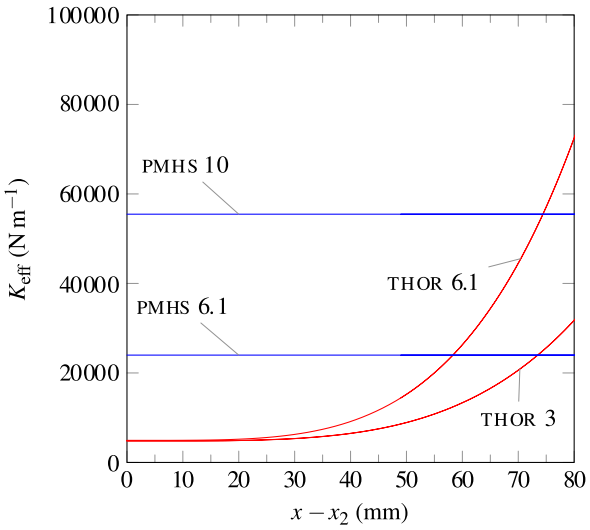

(b) K_{eff} for impactor.

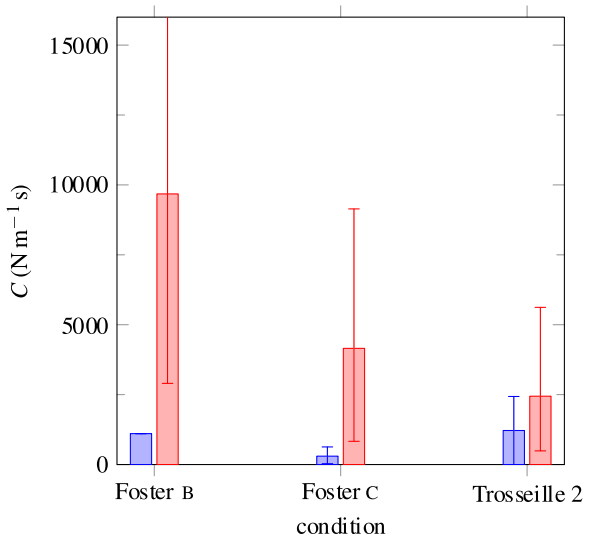

(c) C for seatbelt.

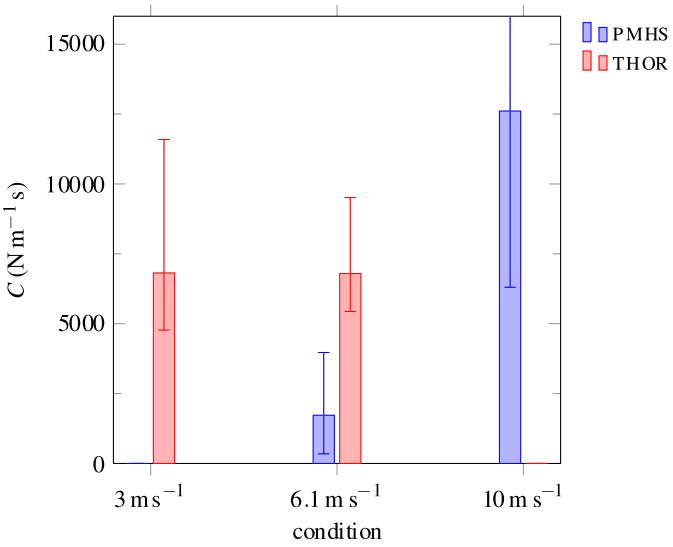

(d) C for impactor.

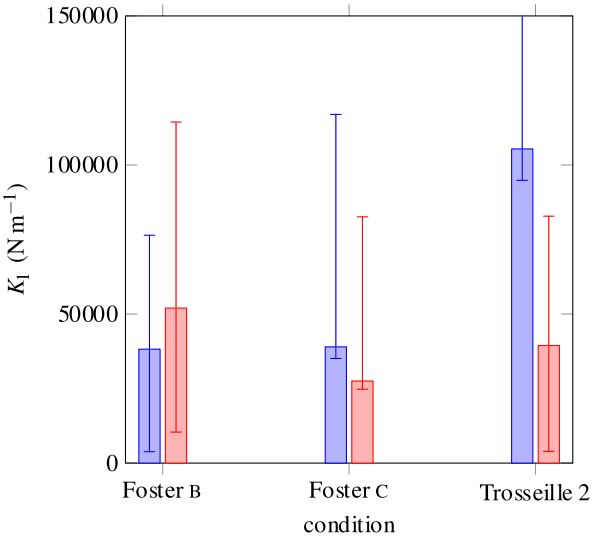

(e) K_1 for seatbelt.

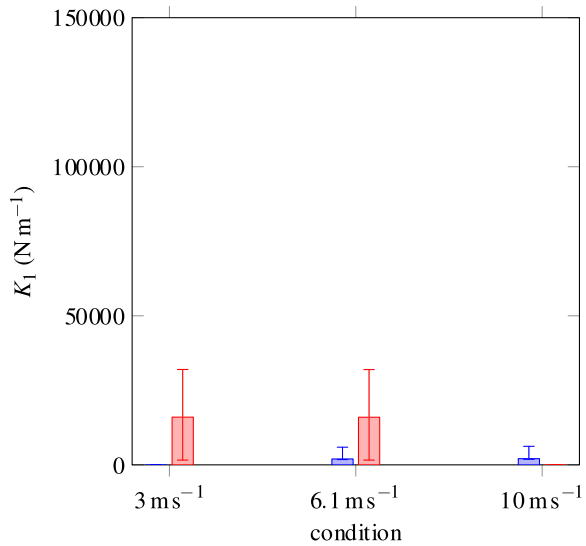

(f) K_1 for impactor.

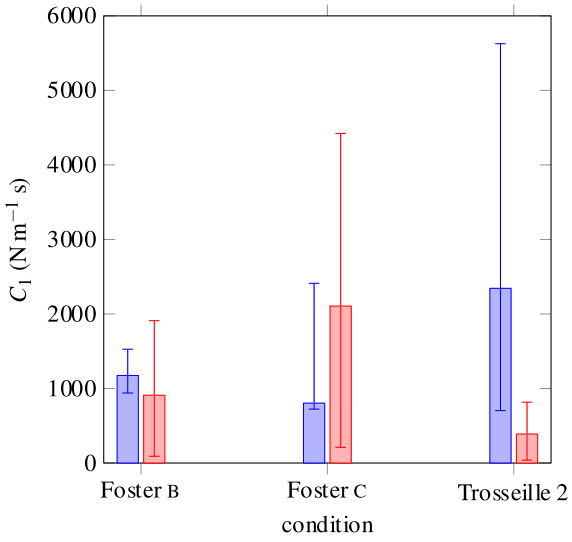

(g) C_1 for seatbelt.

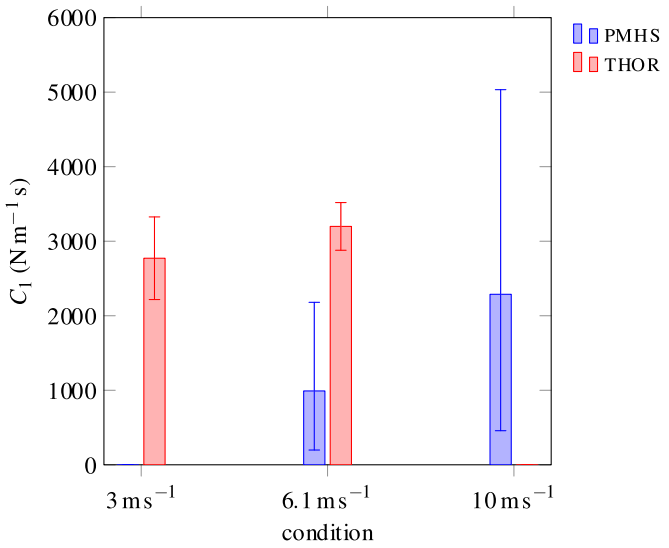

(h) C_1 for impactor.

Fig. 6. Identified model parameters for seatbelt and impactor common loading conditions to PMHS and THOR.
B: B condition from Foster et al. 2006
C: C condition from Foster et al. 2006
2: configuration 2 from Trosseille et al. 2002
PMHS 6.1 m/s: 32 kg 6.1 m/s condition from Cavanaugh et al. 1986
PMHS 10 m/s: 32 kg 10 m/s condition from Cavanaugh et al. 1986
THOR 3 m/s: 32 kg 3 m/s condition from Compigne et al. 2015
THOR 6.1 m/s: 32 kg 6.1 m/s condition from Compigne et al. 2015

IV. DISCUSSION

Interpretation of the results

The parameters values between seatbelt and impactor cases can be compared on Fig. 6. The K values for the PMHS subjects (Fig. 6(a) and (b)) are very different between the seatbelt and impactor cases. Regarding the THOR dummy, the K values for the seatbelt case are the same order of magnitude as the effective stiffness values of the impactor case. The origin value of the THOR curves on Fig. 6(b) is the K_0 value. The linear stiffness of the dummy modelled with a non-linear spring is lower than the stiffness of the other conditions. The C values (Fig. 6(c) and (d)) match well between the seatbelt and impactor cases (except for the 10 m/s condition). K_1 values match between seatbelt and impactor cases for the THOR dummy, whereas values are much lower in the impactor case for the PMHS (Fig. 6(e) and (f)). However, the large range of variation (relative to the optimised value) for the PMHS in the impactor case allows K_1 to take any value to fit the data. C_1 values are similar for PMHS and the THOR dummy (Fig. 6(g) and (h)) between the seatbelt and impactor cases and some large ranges of variation exists.

In order to understand the meaning of the parameters value comparison, one has to note that the influence of the parameters is not the same whether they are placed in series or in parallel in the model. For instance, a spring in parallel will have no effect when its stiffness is equal to 0, whereas a spring in series has no effect when its value tends toward infinity. It is the same for damping parameters. This explains the important range of variation toward high values for K and C concerning PMHS and THOR respectively. A high value for such a component in series means it deforms little. Therefore a higher value means it deforms even less, which does not necessarily change the global result.

The model in series has a characteristic time $\tau = \frac{C}{K}$. The model behaviour is elastic for times inferior to τ and viscous for times superior to τ. The characteristic times have been computed with the optimised K and

C values. It can be concluded that the penetration response of the abdomen is mainly caused by the instantaneous deformation of the spring K for the THOR dummy and by the long-term deformation of the damper C for the PMHS. For the seatbelt case, this is highlighted by Figures A.3. (a) and A.3. (b) (see Appendix), which show the prominence of the K spring and C damper responses on the abdominal penetration of the dummy and the PMHS, respectively. The PMHS characteristic time being low (less than 3 ms) compared to the loading duration, the PMHS response is mainly viscous. On the opposite, the dummy characteristic times are between 20 ms and 80 ms, higher than the loading duration, therefore the response is mainly elastic. Figures A.4. (a) and A.4. (b) (see appendix) show the same phenomenon for the impactor case. It is difficult, however, to compare the characteristic times with a non linear spring in the dummy case.

These findings correlate with the test data reported in [5]. For the impactor case the dummy force response was higher than the PMHS responses and for the seatbelt case the dummy force response was lower than the PMHS responses. This is explained by the previous findings. An impactor loading creates high abdomen penetration, therefore the dummy force response is higher than the PMHS one due to the higher influence of K (the spring non-linearity enhances this phenomenon since high penetration increases the spring force contribution). On the other hand, a seatbelt loading creates less penetration (compared to the impactor loading) and a sharp velocity peak, therefore the dummy force response is lower than the PMHS one due to the lower influence of C.

The fact that the K values are extremely different between the dummy and the PMHS subjects only for the seatbelt case is also explained by the PMHS mainly viscous behaviour for the seatbelt condition, whereas for the impactor condition the spring and damper contribution are more balanced. This may be due to the fact that for the seatbelt condition, the displacement and velocity of the extremity of the model is imposed. The force profile to fit having a similar shape than the velocity profile explains that the K value has less influence. The results would perhaps be different if the force were imposed. In the impactor case, only the initial velocity of the model's extremity is imposed, which imposes less constraints on the model. This also explains why the PMHS K values are higher in the seatbelt case as compared to the impactor case.

This spring-driven behaviour of the dummy and the damper-driven behaviour of the PMHS highlighted by the model are due to the nature of the constitutive material of the human subjects and the dummy. The human abdomen is made of soft tissues that include a large proportion of water, therefore causing a viscous behaviour whereas the dummy abdomen is made of foam and therefore has an elastic behaviour, although not linear and strain rate dependent. The influence of the dummy spine and pelvis (more important than for the human) explains the need for a non-linear spring in the impactor case. The optimised values of the d parameter of the non-linear spring (42 mm and 52 mm) represent the level of compression after which the non-linearity appears. This corresponds to the depth the abdomen foam has to be compressed before the pelvis is involved (measured at approximately 45 mm on the dummy).

Comparison with other studies

References [4] and [10] also developed lumped element models of the abdomen for seatbelt loading. It should be noted that in [4], the penetration of the seatbelt into the abdomen was estimated as the average of the left and right belt strand displacement, although in [11] and [10] the belt penetration in the abdomen was measured directly.

The stiffness parameters found in [4] were from 12000 N/m to 17000 N/m (except for the subject PRT035 showing a very low stiffness) and the damping parameters from 600 N/m.s to 900 N/m.s. The lumped element model used for the THOR dummy in [4] had an extra mass compared to the model used for PMHS and the spring was non-linear. It is difficult to compare those values with the K and C values of this study since the first stage of the present model, where the displacement is imposed, consists of two components in series and not in parallel as in [4]. It was concluded in [4] that the THOR abdomen was too stiff (approximately two times) and not viscous enough (approximately four times) compared to the human subjects. The same conclusion can

be drawn in the present study for K and C, with the distinction that the components are in series in the present model, therefore it is more correct to say that the abdomen response is more influenced by the spring and less by the damper for the dummy compared to the PMHS. It was chosen to compare the parameters of the THOR dummy and the human subjects based on the same lumped element model until it was necessary to use a non-linear spring for the dummy under impactor loading.

Reference [10] applied a lumped element model to PMHS response under seatbelt loading. But as the front stage of the model had K and C in parallel it is difficult to compare their values with those from the present model. Non-linear elements were used for K, K_1 and C_1, which also makes it difficult to compare them with the values from this study. Moreover, in [10] the force from test data was applied to the model and the penetration given by the model was compared with the test data. This is a different approach from the one used in this study, where the penetration was applied to the model, as in [4] and [8], which is believed to be more representative of a seatbelt loading with a piston or pretensioners. The two different methods could potentially lead to different results with the same parameters, especially in cases where the elements of the model are non-linear.

There is also a difference in the manner of determining the value of the parameters for given reference data. In [4] and [10] the parameters were identified from the test data as sloped in a force-penetration diagram for a stiffness parameter, for example. In this study an optimisation procedure was used, as in [7] and [9]. A sensitivity analysis of the optimised parameters was also performed to predict the effect of the variation of the parameters on the response of the model.

Limitations

Lumped element models applied to impact biomechanics have inherent limitations. They only represent a one-dimensional loading and use simple mechanical parameters. A linear model proved to be sufficient to fit the PMHS and dummy response until non linearity appeared for dummy impactor tests. The structure chosen for the first stage of the present model (Maxwell model) theoretically represents a fluid behaviour. If loaded with an imposed constant force (like at the end of a seatbelt loading, for instance), it would result in an infinitely increasing penetration. A generalised Maxwell model with three elements (standard linear solid) would account for those limitations.

As described above, the second stage of the model contributes less to the global penetration response of the model. This causes the K_1 and C_1 parameters to have less influence on the response and more variability than the K and C parameters. This limits the relevance of a two stages model.

The fact that for the PMHS subjects in the impactor case the model penetration is higher than the penetration from test data raises a limitation of the model. The penetration is not imposed on the model, unlike for the seatbelt case, and since the model parameters are optimised to fit the force from test data only, the penetration response of the model does not necessarily fit the test data. This could be due to the fact that the model does not take into account the abdomen depth, therefore allowing the predicted penetration to be higher than the test penetration. This could also be due to the Maxwell model used for the first stage of the model, where the C damping element does not unload. This can be seen on Fig. A.4. (b) where the compression of C does not decrease during unloading. It would also be useful to have abdomen depth considered in the lumped element model to account for the individual anthropometry variations between PMHS subjects.

Guidelines for improving the THOR dummy

Although there are differences in the model parameters values between the seatbelt and impactor case, the results show that the THOR dummy abdomen is more elastically and less viscously deformable compared to the human abdomen. This behaviour is mainly explained by the first stage of the model, i.e. related to parameters K and C since the second stage contributes less to the response as explained above.

Based on these observations, some improvements can be applied to the dummy at the material and structural levels. The material properties of the lower abdomen foam should be modified to favour the viscous behaviour instead of the elastic behaviour. The need of a non-linear spring for the dummy model at high penetrations, whilst it was not necessary for the PMHS, means that stiffer parts (such as the pelvis) contribute non-biofidelically more to the response than soft parts. This confirms the design changes of this region implemented on THOR Mod Kit, which shortened the pelvis flesh at antero-superior iliac spines by around 20 mm. Furthermore, the difference in moving mass between the dummy abdomen and the PMHS has an influence and therefore the dummy abdomen mass should be increased.

V. CONCLUSION

A lumped element model has been designed in order to reproduce the abdomen force-penetration response of human subjects and the THOR dummy under seatbelt and impactor loading. This model proved to be capable of fitting the different test data and allows an explanation of the differences between the abdomen response of human subjects and a crash test dummy in terms of mechanical parameters. The viscous contribution to the dummy abdomen deformation has to be increased relative to the elastic contribution in order to improve its biofidelity. To achieve this goal, the material and structural modifications of THOR abdomen proposed in this study will be tested on THOR Metric FE model released by NHTSA in 2015 (v2.1). The ultimate goal will be to propose a new abdomen prototype.

VI. ACKNOWLEDGEMENTS

The authors would like to thank Messrs Philippe Petit and Xavier Trosseille for allowing to use data from Trosseille et al. 2002 and from Lamielle et al. 2008 as well as Mr Craig Foster for providing the data from Foster et al. 2006.

VII. REFERENCES

[1] Elhagediab, A. and Rouhana, S. Patterns of Abdominal Injury in Frontal Automotive Crashes. *16th International Technical Conference on the Enhanced Safety of Vehicles*, 1998, Windsor (Canada). Number 98-S1-W-26.

[2] Martin, J.-L., Lardy, A. and Compigne, S. Specificities of Rear Occupant Protection: Analysis of French Accident Data. *Proceedings of IRCOBI Conference Proceedings*, 2010, Hanover (Germany).

[3] Frampton, R., Lenard, J. and Compigne, S. An In-depth Study of Abdominal Injuries Sustained by Car occupants in Frontal Crashes. *56th AAAM Annual Conference — Ann Adv Automot Med*, 2012, 56:137–149.

[4] Trosseille, X., Le-Coz, J.-Y., Potier, P. and Lassau, J.-P. Abdominal Response to High-Speed Seatbelt Loading. *Stapp Car Crash Journal*, 2002, 46:71-79. number 2002-22-0004.

[5] Compigne, S., Masuda, M., Hanen, G., Vezin, P., and Bermond, F. Proposal for a Modified THOR Lower Abdomen Including Abdominal Pressure Twin Sensors. *24th International Technical Conference on the Enhanced Safety of Vehicles*, 2015, Gothenburg (Sweden). Number 15-0216.

[6] Hanen, G., Bermond, F., Compigne, S. and Masuda, M. Contribution to the Improvement of Crash Test Dummies in Order to Decrease Abdominal Injuries in Road Accidents. *22nd International Technical Conference on the Enhanced Safety of Vehicles*, 2011, Washington D.C. (USA). Number 11-0218.

[7] Lobdell, T., Kroell, C., Schneider, D., Hering, W. and Nahum, A. Impact Response of the Human Thorax. *Human Impact Response: Measurement and Simulation*, pp. 201–245, eds W. King and H. Mertz, 1973. *Proceedings of the Symposium on Human Impact Response*, Warren (USA), October 2-3, 1972.

[8] Kent, R., Lessley, D. and Sherwood, C. Thoracic Response to Dynamic, Non-Impact Loading from a Hub, Distributed Belt, Diagonal Belt, and Double Diagonal Belts. *Stapp Car Crash Journal*, 2004, 48:495-519. Number 2004-22-0022.

[9] Parent, D., Craig, M., Ridella, S. and McFadden, J. Thoracic Biofidelity Assessment of the THOR MOD KIT ATD. *23rd International Technical Conference on the Enhanced Safety of Vehicles*, 2013, Seoul (Korea). Number 13-0327.

[10] Lamielle, S., Vezin, P., Verriest, J.-P., Petit, P., Trosseille, X. and Vallancien, G. 3D Deformation and Dynamics of the Human Cadaver Abdomen under Seatbelt Loading. *Stapp Car Crash Journal*, 2008, 52:267-294. Number 2008-22-0014.

[11] Foster, C., Hardy, W., Yang, K., King, A. and Hashimoto, S. High-Speed Seatbelt Pretensioner Loading of the Abdomen. *Stapp Car Crash Journal*, 2006, 50:27-51. Number 2006-22-0002.

[12] Cavanaugh, J., Nyquist, G., Goldberg, S. and King, A. Lower Abdominal Tolerance and Response. *30th Stapp Car Crash Conference Proceedings*, San Diego (USA), 1986. Number 861878.

[13] Hardy, W., Schneider, L. and Rouhana, S. Abdominal Impact Response to Rigid-Bar, Seatbelt, and Airbag Loading. *Stapp Car Crash Journal*, 2001, 45. Number 2001-22-0001.

[14] Shigeta, K., Kitagawa, Y. and Yasuki, T. Development of Next Generation Human FE Model Capable of Organ Injury Prediction. *21st International Technical Conference on the Enhanced Safety of Vehicles*, 2009, Stuttgart (Germany). Number 09-0111.

[15] Untaroiu, C., Lim, J.-Y., Shin, J., Crandall, J., Malone, D. and Tannous, R. Evaluation of a Finite Element Model of the THOR-NT Dummy in Frontal Crash Environment. *21st International Technical Conference on the Enhanced Safety of Vehicles*, 2009, Stuttgart (Germany). Number 09-0272.

[16] GESAC, Inc. Test Support for Finite Element Modeling of THOR Crash Test Dummy. 1999. Submitted to Volpe National Transportation System Center.

[17] GESAC, Inc. Thor NT Advanced Frontal Impact Dummy Internet: www.gesacinc.com/thornt.html, Date Updated 30 January 2015.

[18] Xu, L., Agaram, V., Rouhana, S., Hultman, R., Kostyniuk, G., McCleary, J., Mertz, H.,Nusholtz, G. and Scherer R. Repeatability Evaluation of the Pre-Prototype NHTSA Advanced Dummy Compared to the Hybrid III. SAE World Congress, Detroit (USA), 2000. Number 2000-01-0165.

VIII. APPENDICES

TABLE A.I.

IDENTIFIED PARAMETERS FOR SEATBELT LOADING CONDITIONS, INCLUDING SENSITIVITY ANALYSIS

(PARAMETERS VALUE RANGE WHICH KEEPS GOODNESS OF FIT PARAMETERS WITHIN ±10% RANGE)

		Trosseille et al. 2002 condition 2					
		K (N/m)	C (N/m.s)	K_1 (N/m)	C_1 (N/m.s)	M (kg)	m (kg)
PMHS	superior limit	1350054	1217	210787	3282	10.2	1
	optimised value	**900036**	**1217**	**105393**	**2344**	**6**	**0.5**
	inferior limit	630025	1217	10539	1641	1.8	0.05
		Foster et al. 2006 B condition					
		K	C	K_1	C_1	M	m
	superior limit	1140043	1107	76428	1527	9.6	1.6
	optimised value	**570021**	**1107**	**38214**	**1175**	**6**	**1**
	inferior limit	342013	1107	3821	940	3	0.3
		Foster et al. 2006 C condition					
		K	C	K_1	C_1	M	m
	superior limit	1692911	330	77983	1608	12	1.1
	optimised value	**846456**	**300**	**38992**	**804**	**6**	**1**
	inferior limit	423228	270	3899	80	1.2	0.9

	Trosseille et al. 2002 condition 2						
		K	C	K_1	C_1	M	m
	superior limit	137326	3178	43387	428	0.4	0.2
	optimised value	**124841**	**2445**	**39443**	**389**	**0.2**	**0.1**
	inferior limit	112357	1956	35499	350	0.02	0.01
	Foster et al. 2006 B condition						
		K	C	K_1	C_1	M	m
THOR	superior limit	125792	19356	62396	1000	0.4	0.2
	optimised value	**114357**	**9678**	**51997**	**910**	**0.2**	**0.1**
	inferior limit	102921	6774	41597	819	0.02	0.01
	Foster et al. 2006 C condition						
		K	C	K_1	C_1	M	m
	superior limit	104873	4986	55076	2317	0.4	0.2
	optimised value	**95339**	**4155**	**27538**	**2106**	**0.2**	**0.1**
	inferior limit	85805	3324	2754	1896	0.02	0.01

TABLE A.II.

IDENTIFIED PARAMETERS FOR IMPACTOR LOADING CONDITIONS, INCLUDING SENSITIVITY ANALYSIS (PARAMETERS VALUE RANGE WHICH KEEPS GOODNESS OF FIT PARAMETERS WITHIN ±10% RANGE)

	Cavanaugh et al. 1986 32 kg 6.1 m/s condition								
			K (N/m)	C (N/m.s)	K_1 (N/m)	C_1 (N/m.s)	M (kg)	m (kg)	m_b (kg)
	superior limit		31179	2244	3949	1189	9	2	110
	optimised value		**23984**	**1726**	**1974**	**991**	**6**	**1**	**55**
	inferior limit		21585	1381	197	793	3	0.1	33
	Cavanaugh et al. 1986 32 kg 10 m/s condition								
			K	C	K_1	C_1	M	m	m_b
	superior limit		66570	25217	4149	2746	10.8	2	154
	optimised value		**55475**	**12609**	**2075**	**2288**	**6**	**1**	**77**
PMHS	inferior limit		49928	6304	207	1830	1.2	0.1	53.9
	Hardy et al. 2001 48 kg 6 m/s condition								
			K	C	K_1	C_1	M	m	m_b
	superior limit		37220	1384	81092	5847	12	2	80.4
	optimised value		**37220**	**1259**	**40546**	**2923**	**6**	**1**	**67**
	inferior limit		37220	1133	4055	1462	0.6	0.1	60.3
	Hardy et al. 2001 48 kg 9 m/s condition								
			K	C	K_1	C_1	M	m	m_b
	superior limit		73832	3338	20284	1873	9.6	2	74.1
	optimised value		**67120**	**2781**	**10142**	**1561**	**6**	**1**	**57**
	inferior limit		60408	2225	1014	1249	1.8	0.1	45.6
	Compigne et al. 2015 32 kg 3 m/s condition								
		K_0 (N/m)	d (mm)	p (no unit)	C (N/m.s)	K_1 (N/m)	C_1 (N/m.s)	M (kg)	m (kg)	m_b (kg)
	superior limit	5284	52	4	11588	32005	3326	0.4	0.2	101.4
	optimised value	**4804**	**52**	**4**	**6817**	**16002**	**2772**	**0.2**	**0.1**	**78**
THOR	inferior limit	4323	52	4	4772	1600	2217	0.02	0.01	62.4
	Compigne et al. 2015 32 kg 6.1 m/s condition									
		K_0	d	p	C	K_1	C_1	M	m	m_b
	superior limit	6911	42	4	9514	31955	3519	0.4	0.2	109.2
	optimised value	**4936**	**42**	**4**	**6796**	**15977**	**3199**	**0.2**	**0.1**	**78**
	inferior limit	3949	42	4	5437	1598	2879	0.02	0.01	62.4

TABLE A.III.

ANTHROPOMETRY OF CONSIDERED PMHS SUBJECTS

	Trosseille et al. 2002						
	configuration	test	gender	age (years)	body mass (kg)	stature (cm)	abdomen depth (mm)
seatbelt	2	PRT038	F	64	45	149	206
		PRT039	F	86	50	150	207
	Foster et al. 2006						
	configuration	test	gender	age (years)	body mass (kg)	stature (cm)	abdomen depth (mm)
	B	B-1	M	85	81	169	360
		B-2	M	45	75	174	258
		B-3	M	59	62	169	261
	C	C-1 C-2	F	86	38	159	191
	Cavanaugh et al. 1986						
	configuration	test	gender	age (years)	body mass (kg)	stature (cm)	abdomen depth (mm)
impactor	low velocity	14	M	56	68	182	283
		19	F	43	53	159	231
		24	M	57	45	187	257
		28	F	57	75	163	275
		33	F	51	68	163	261
	high velocity	37	M	50	88	169	332
		57	M	64	90	184	322
		61	M	60	79	180	277

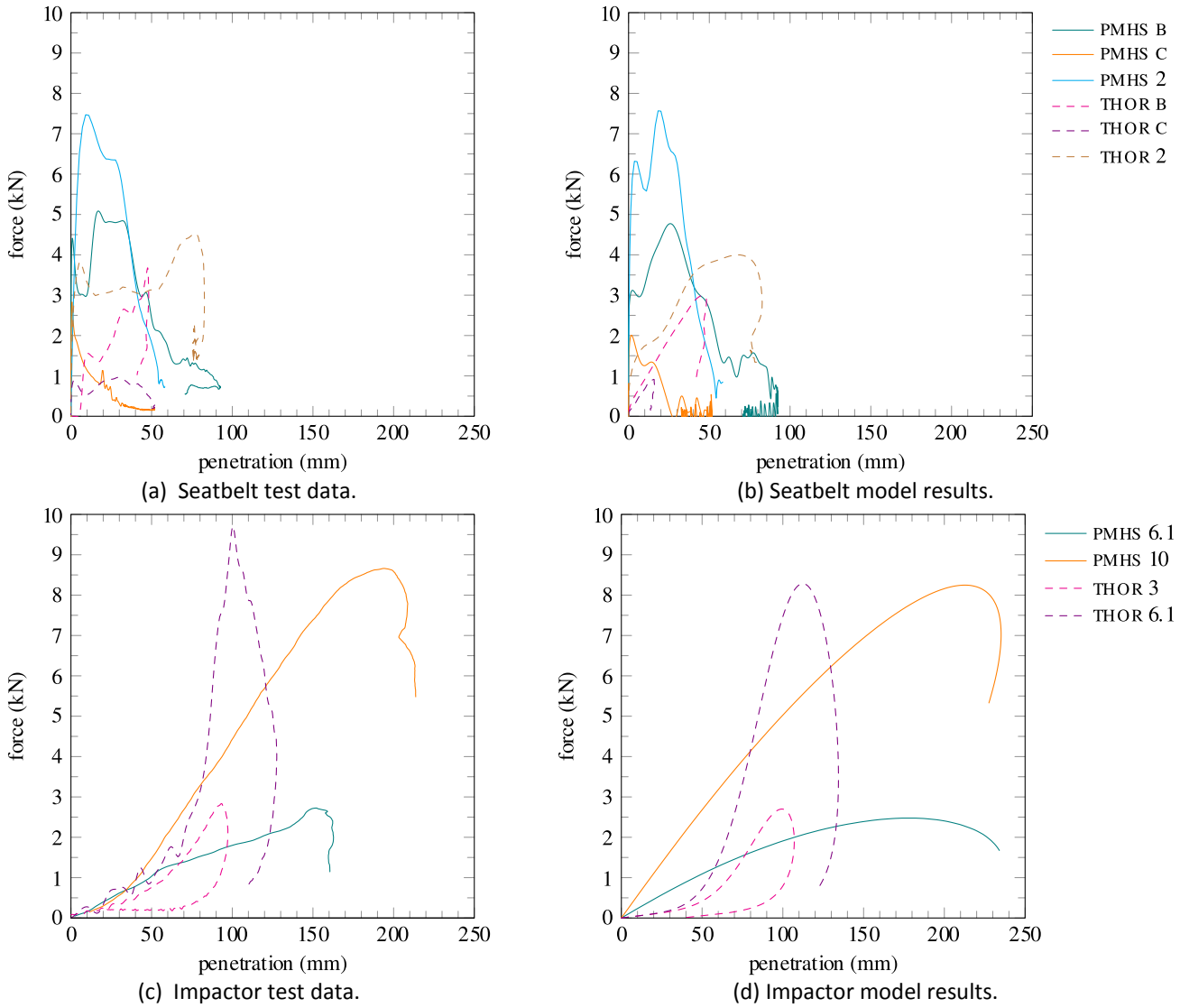

(a) Seatbelt test data.

(b) Seatbelt model results.

(c) Impactor test data.

(d) Impactor model results.

Fig. A.1. Force-penetration responses.

B: B condition from Foster et al. 2006

C: C condition from Foster et al. 2006

2: configuration 2 from Trosseille et al. 2002

PMHS 6.1 m/s: 32 kg 6.1 m/s condition from Cavanaugh et al. 1986

PMHS 10 m/s: 32 kg 10 m/s condition from Cavanaugh et al. 1986

THOR 3 m/s: 32 kg 3 m/s condition from Compigne et al. 2015

THOR 6.1 m/s: 32 kg 6.1 m/s condition from Compigne et al. 2015

485

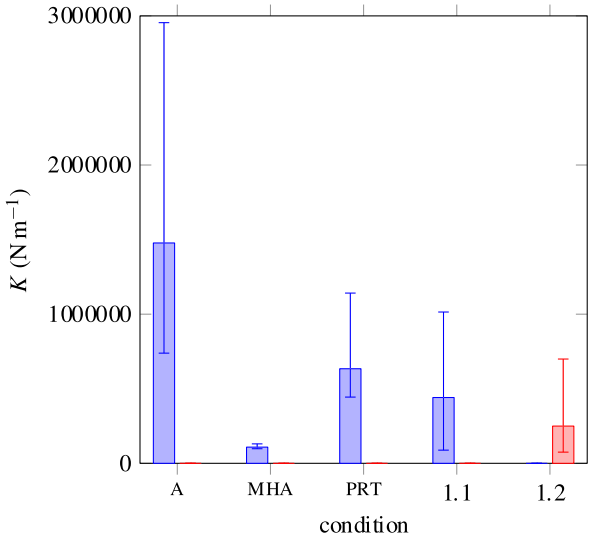

(a) K for seatbelt.

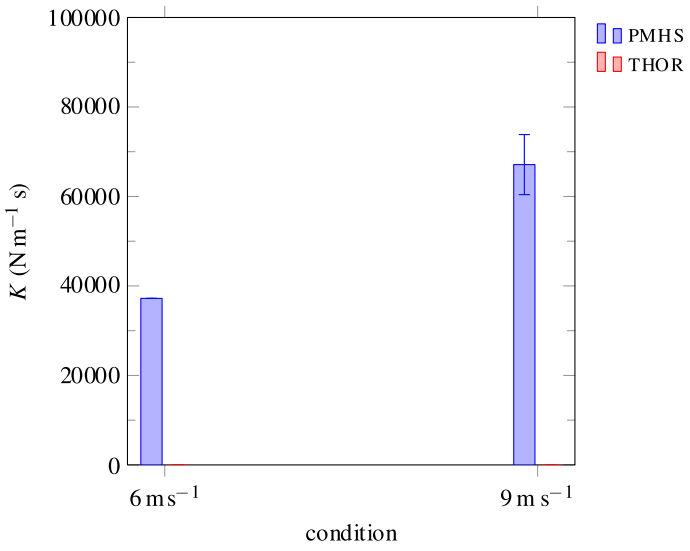

(b) K_{eff} for impactor.

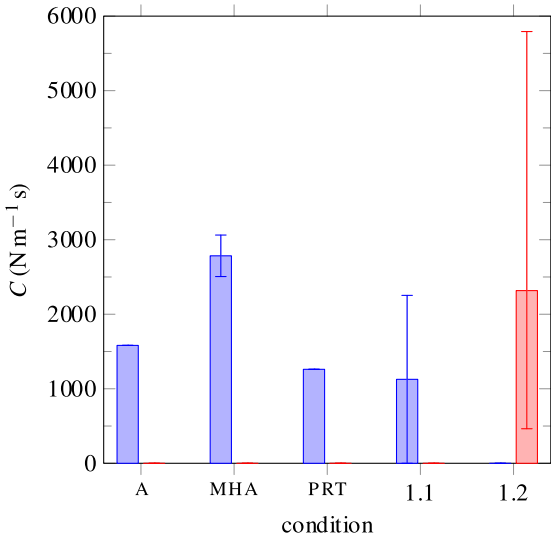

(c) C for seatbelt.

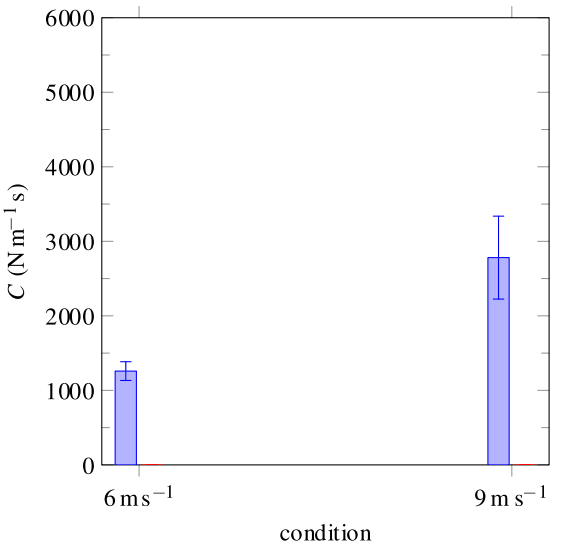

(d) C for impactor.

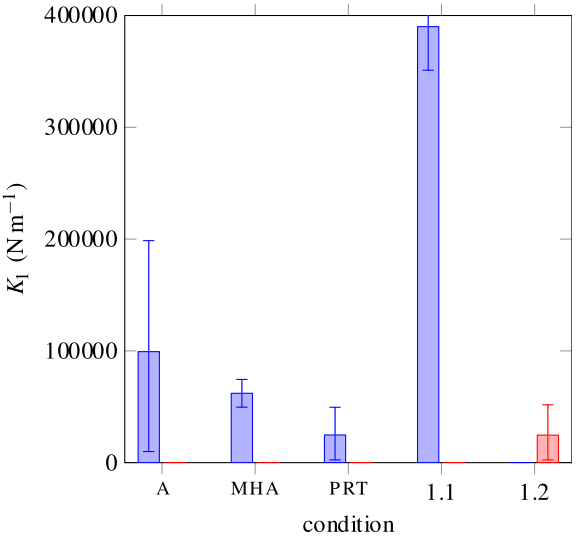

(e) K_1 for seatbelt.

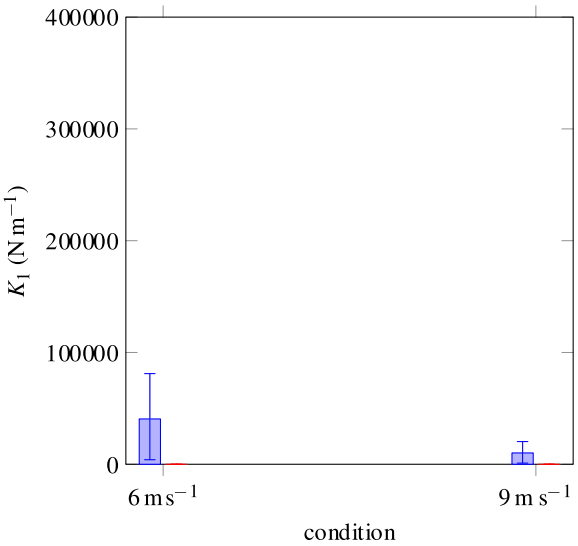

(f) K_1 for impactor.

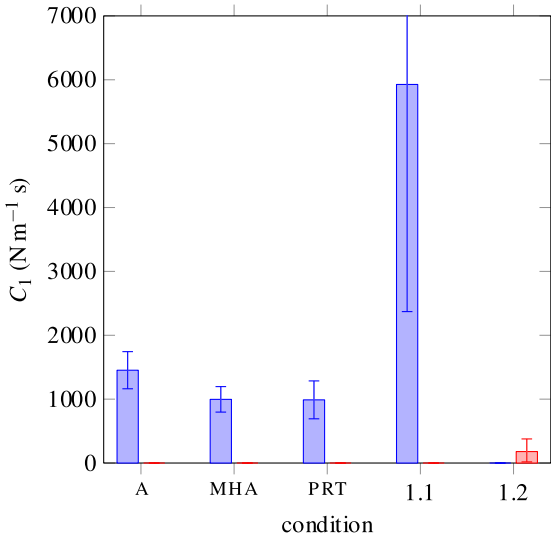

(g) C_1 for seatbelt.

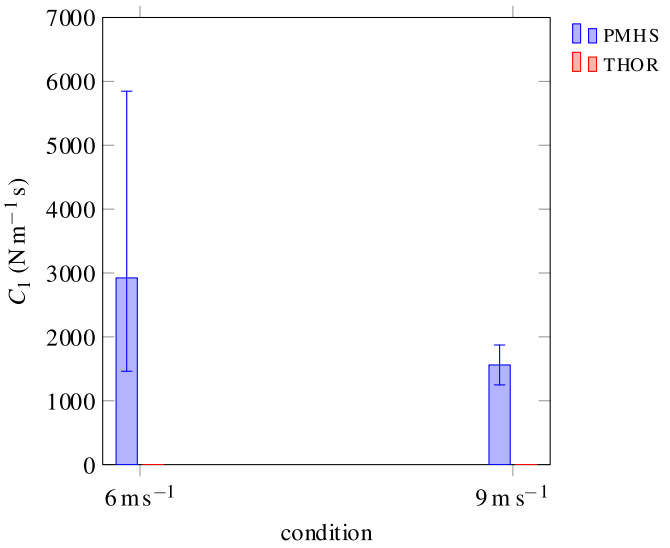

(h) C_1 for impactor.

Fig. A.2. Identified model parameters for additional seatbelt and impactor loading conditions.
A: A condition from Foster et al. 2006
MHA: MHA condition from Lamielle et al. 2008
PRT: PRT condition from Lamielle et al. 2008
1.1: configuration 1 from Trosseille et al. 2002 (PMHS)
1.2: configuration 1 from Trosseille et al. 2002 (THOR)
PMHS 6 m/s: 48 kg 6 m/s condition from Hardy et al. 2001
PMHS 9 m/s: 48 kg 9 m/s condition from Hardy et al. 2001

486

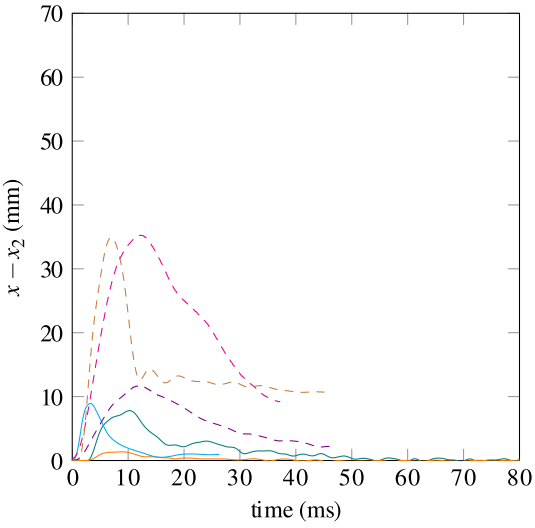

(a) Deformation of K spring.

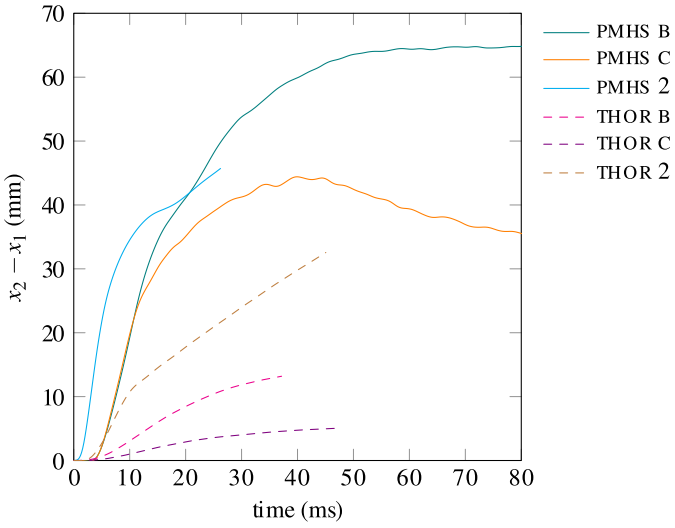

(b) Deformation of C damper.

Fig. A.3. Displacement results for seatbelt loading conditions.
B: B condition from Foster et al. 2006
C: C condition from Foster et al. 2006
2: configuration 2 from Trosseille et al. 2002

487

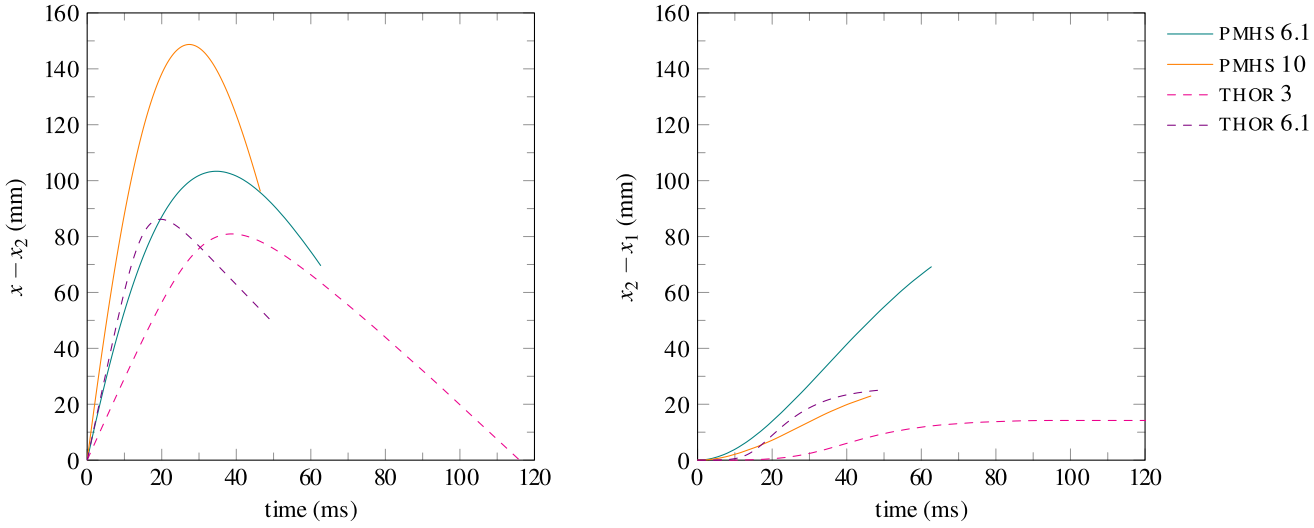

(a) Deformation of K spring.

(b) Deformation of C damper.

Fig. A.4. Displacement results for impactor loading conditions.
PMHS 6.1 m/s: 32 kg 6.1 m/s condition from Cavanaugh et al. 1986
PMHS 10 m/s: 32 kg 10 m/s condition from Cavanaugh et al. 1986
THOR 3 m/s: 32 kg 3 m/s condition from Compigne et al. 2015
THOR 6.1 m/s: 32 kg 6.1 m/s condition from Compigne et al. 2015